
A Dissection of Overfitting and Generalization in Continuous Reinforcement Learning

Amy Zhang
McGill University
Facebook AI Research
amyzhang@fb.com

Nicolas Ballas
Facebook AI Research
ballasn@fb.com

Joelle Pineau
McGill University
Facebook AI Research
jpineau@fb.com

Abstract

The risks and perils of overfitting in machine learning are well known. However most of the treatment of this, including diagnostic tools and remedies, was developed for the supervised learning case. In this work, we aim to offer new perspectives on the characterization and prevention of overfitting in deep Reinforcement Learning (RL) methods, with a particular focus on continuous domains. We examine several aspects, such as how to define and diagnose overfitting in MDPs, and how to reduce risks by injecting sufficient training diversity. This work complements recent findings on the brittleness of deep RL methods and offers practical observations for RL researchers and practitioners.

1 Introduction

Machine learning is concerned with learning a function from data. That data typically consists of a mix of *pattern* and *noise*. For most supervised learning applications, the data comes from the natural world, where the pattern may be (near) infinitely complex, and the true noise is not known. Yet recent studies on generalization in **supervised learning** have shown that deep neural networks, with their overparameterization and massive capacity, can lead to memorization of the data, and thus poor generalization [Zhang et al., 2018, Arpit et al., 2017].

One of the objectives of our work is to explore if similar issues occur in **reinforcement learning** (RL). Indeed, recent findings have shown significant brittleness of deep RL methods [Henderson et al., 2018]. One of the challenges with RL, is that almost all research is done using simulators. By design, these simulators consist of finite and stationary lines of code, running a deterministic program, where the only injection of *noise* is through an initial random seed. In this case, it is not surprising that (for a fixed random seed), given sufficient data, the RL method will exhaust the noise. In effect, memorization is inevitable. This is especially prevalent in simple tasks, those with small state spaces, simple perception, short planning horizon, and deterministic transition functions. This constitutes a large portion of benchmark domains considered in the field [Brockman et al., 2016, Machado et al., 2017, Beattie et al., 2016].

In this work we examine conditions under which deep RL achieves generalization vs memorization, with both model-free and model-based reinforcement learning methods. We investigate the prevalence of memorization with randomization experiments in both the discrete and continuous action setting, as well as with value-based and policy-based methods. Through randomized reward experiments,

we develop strategies to test memorization. We also propose tests to investigate robustness of the learned policy specific to the continuous domain, by expanding the initial state distribution and adding stochastic noise to the observation space.

We first explore classic RL simulated environments such as the Cartpole and Acrobot control tasks in the Gym toolkit [Brockman et al., 2016] with discrete action space and also look at the continuous action space setting with MuJoCo Reacher and Thrower environments [Todorov et al., 2012]. As the goal of RL is eventually to transfer to the real world, we propose new reinforcement learning tasks that received observations from natural images and explore generalization in that setting as well.

Our analysis shows that deep RL algorithms can overfit both in standard simulated environment and when operating on natural images. However, as soon as there is enough training data diversity in the simulated environment, deep RL generalizes well. It is likely due to the fact that these commonly used synthetic domains have relatively little noise and spurious patterns. On the other hand, deep RL algorithms show more prominent overfitting when observing natural data. Those observations advocate for the development of new benchmarks in order to study more thorough overfitting in deep RL.

2 Technical Background

Reinforcement Learning. We examine the setting where the environment is a Markov Decision Process (MDP), represented by a tuple $M = (\mathcal{S}, \mathcal{A}, T, R, S_0, \gamma)$, where \mathcal{S} is a state space, \mathcal{A} an action space, $T(s, a, s')$ is the state-to-state transition distribution with $s, s' \in \mathcal{S}$, $R(s, a)$ is the reward function, S_0 the initial state distribution, $\gamma \in [0, 1)$ a discount factor [Bellman, 1957]. The policy $\pi : \mathcal{S} \rightarrow \mathcal{A}$ defines an action selection strategy. Reinforcement learning (RL) is concerned with finding an optimal policy, denoted $\pi^* : \mathcal{S} \rightarrow \mathcal{A}$, that maximizes the expected sum of rewards.

Value function estimation. The value function defines the expected sum of rewards over the trajectory $t = 0 \dots T$ while following policy π : $V^\pi(s) = \mathbb{E}[\sum_{t=0}^T \gamma r_t | s_0 = s]$. The state-action Q-function is similarly defined and can be recursively estimated from Bellman’s equation: $Q^\pi(s_t, a_t) = r_t + \gamma \sum_{s' \in \mathcal{S}} T(s, a, s') \max_{a' \in \mathcal{A}} Q(s', a')$.

In the absence of a known transition model $T()$, the Q-function can be estimated from a batch of data using fitted Q-iteration, which learns an approximate function $\hat{Q}(\cdot, \theta)$, parameterized by θ , minimizing the loss: $\mathcal{L}(\theta) = \left(\hat{Q}(s_t, a_t, \theta) - Y_t \right)^2$, where $Y_t = r_t + \gamma \max_a Q(s_{t+1}, a, \theta)$.

Deep RL. The Deep Q-Network (DQN) extends fitted Q-iteration by using a (potentially large) neural network for the Q-function [Mnih et al., 2015]. Several additional steps are helpful in stabilizing learning, including using a target network from a previous iteration, applying L1-smoothing of the loss, incorporating experience replay [Mnih et al., 2015], and correcting with Double DQN [van Hasselt et al., 2015]. This class of approach is suitable for continuous state, discrete action MDPs.

Policy-based Methods. In the case of continuous action domains, policy-based methods are typically used. Here we directly estimate a parameterized form of the optimal policy $\pi_\theta(s)$, where in deep RL $\pi_\theta(s)$ takes the form of a neural network. This network takes as input the state s_t , outputs a distribution over possible actions a_t , and is trained with a loss of the form: $\mathcal{L}_{PG}(\theta) = \mathbb{E}_t [\log \pi_\theta(a_t | s_t) \hat{A}^\pi(s_t, a_t)]$. Proximal Policy Optimization (PPO) [Schulman et al., 2017] is a popular variant of policy gradient methods that incorporates constraints on the policy change, as well as mini-batches and multiple epochs of learning between each query of the environment.

3 Perspectives on generalization and overfitting

3.1 Generalization in Supervised Learning

In Supervised Learning (SL), we assume an unknown data distribution \mathcal{D} from which we draw i.i.d samples $\mathcal{X}_{\text{train}}$ with ground truth labels $\mathcal{Y}_{\text{train}}$ where $y \in \mathcal{Y}$ are extracted from a target concept $y = c(x)$. The goal is to learn a function f that learns the mapping from $\mathcal{X}_{\text{train}}$ to $\mathcal{Y}_{\text{train}}$. Given a loss function $l(f(x), y)$, the generalization error E_G is defined as the difference in true and expected error.

$$E_G = E_{x,y \sim \mathcal{D}}[l(f(x), y)] - \frac{1}{N} \sum_{i=1}^N l(f(x_{tr,i}), y_{tr,i}) \quad (1)$$

In practice, however, we do not have access to underlying joint probability distribution $p(x, y)$. Instead, we compute a proxy empirical error using a withheld test set $(\mathcal{X}_{\text{test}}, \mathcal{Y}_{\text{test}})$ drawn from the same distribution as $(\mathcal{X}_{\text{train}}, \mathcal{Y}_{\text{train}})$. This gives us the following formula for generalization error:

$$E_G = \frac{1}{M} \sum_{i=1}^M l(f(x_{te,i}), y_{te,i}) - \frac{1}{N} \sum_{i=1}^N l(f(x_{tr,i}), y_{tr,i}) \quad (2)$$

where $N = |\mathcal{X}_{\text{train}}|$, $M = |\mathcal{X}_{\text{test}}|$, $(x_{tr,i}, y_{tr,i}) \in (\mathcal{X}_{\text{train}}, \mathcal{Y}_{\text{train}})$, and $(x_{te,i}, y_{te,i}) \in (\mathcal{X}_{\text{test}}, \mathcal{Y}_{\text{test}})$. **Overfitting** is defined as poor generalization behavior, or large E_G .

Recent work [Zhang et al., 2016] explores the issue of generalization performance in the supervised setting, showing that deep neural networks are capable of memorizing random data, thus exhibiting extreme overfitting.

An interesting question is whether analogous concepts of generalization, memorization and overfitting arise in the reinforcement learning framework.

3.2 Generalization and Memorization in Reinforcement Learning

We focus on characterizing and diagnosing overfitting in deep Reinforcement Learning (RL) methods, with a specific focus on continuous domains. The continuous state space case is particularly interesting with deep reinforcement learning because it is a setting where we expect function approximation (and particularly, a function represented by a deep neural network) to perform well. The continuous state setting is also interesting because we cannot feasibly explore all possible initial states during training time, thus we suppose that generalization is necessary to solve the task¹.

Considering the fact that almost all research in RL is done using simulators, to further examine generalization and overfitting it is necessary to consider cases where (1) the dataset is much smaller than the complexity of the simulator, (2) the random seed is varied to create noise (thus inducing variance in the trajectories due to different initial states or transitions), or alternately (3) the simulator itself is drawn from a random distribution (e.g. by varying the initial state distribution, or transition function, or reward function). We investigate all three cases in experiments below. Cases 1 & 2 correspond to within-task generalization; case 3 corresponds to out-of-task (or transfer) generalization.

In the within-task case, generalization is achieved when a policy trained on an initial set of training trajectories is shown to perform well on a set of test trajectories generated by the same simulator. In the out-of-task case, generalization is achieved when a policy trained on one setting of the simulator performs well on another setting of the simulator.

As exposed above, the only source of noise when doing RL in a simulated environment is through the random seed. Thus, as also proposed in Zhang et al. [2018], the only way to achieve a separation between *training* and *testing* sets is by separation of random seeds. Define $\mathcal{S}_{0,train}$ to be the trajectories generated by the set of training seeds, and $\mathcal{S}_{0,test}$ to be the set of trajectories generated by the testing seed.

We can now define generalization in RL:

$$E_{G,RL} = \frac{1}{N} \sum_{i=1}^N \sum_{t=1}^T R(s_t, \pi_\theta(s_t) | s_0 = s_{tr,i}) - \frac{1}{M} \sum_{i=1}^M \sum_{t=1}^T R(s_t, \pi_\theta(s_t) | s_0 = s_{te,i}), \quad (3)$$

where N is the number of training seeds, M is the number of test seeds, $s_{tr,i} \in \mathcal{S}_{0,train}$, $s_{te,i} \in \mathcal{S}_{0,test}$, T is the length of each episode, and π_θ is our parameterized policy in the policy-based method case, and $\pi_\theta = \arg \max_a Q_\theta(s, a)$ in the value-based method case. In practice, for all of our experiments, we fix the number of test seeds to be $M = 100$.

In addition to simulated environments, we also propose new tasks where observations are grounded in natural data. We investigate deep-RL generalization behaviors on tasks where noise comes from a natural source in that setting.

¹Our work was done concurrently with Zhang et al. [2018], which focuses on the discrete state setting.

4 Overfitting and memorization in the within-task case

In this section we perform a series of empirical demonstrations to illustrate the various incarnations of overfitting in RL. Several details of the experimental setup, including domain specification, deep learning architecture and training regime are included in the appendix. They are not necessary to understand the main findings, but may be useful for reproducing the work.

4.1 On the effect of the number of training random seeds

Consider the case where we fix the number test seeds to $M = 100$ and vary the number of training seeds. We track the difference in performance on the initial state drawn from the set of train seeds vs. the set of test look at the difference in performance.

Discrete Action Space. Experiments with discrete action spaces use a Double DQN architecture. Full implementation details are in the appendix and code will be released. We first consider the popular Acrobot task [Sutton, 1996]. We look at 2 versions of this domain: a first where the state space is defined over the 6-dimensional joint position & velocity space, and a second where the state is described in pixel space from a visual representation of the domain. In the pixel case we concatenate multiple consecutive screens to allow velocity estimation, and thus circumvent partial observability. Figure 1 shows overfitting in both representations, for smaller number of training seeds². When the number of training seeds gets to be around 10, there is sufficient diversity in training data to generalize well given the simplicity of the environment.

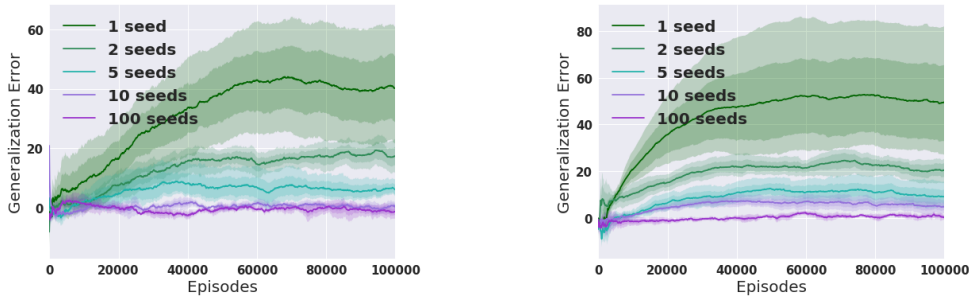


Figure 1: The 6-dim Acrobot (left) and Pixel Acrobot (right), varying number of train seeds from 1 to 100, with $\gamma = 0.99$. Averaged over 5 runs. Trained for 10K episodes (6-dim) and 100K episodes (Pixel).

Next we consider the ubiquitous Cartpole domain. Again, we investigate using the standard 4-dimensional state space (position and velocity of the cart, plus angle and angular velocity of the pole). We also consider Pixel Cartpole, which uses a visual representation of the task. For this domain, looking at Fig. 2, we do not see any overfitting with the lower dimensional representation. However overfitting is clearly seen in the Pixel Cartpole case.

In both domains, by controlling the number of seeds drawn from the initial state distribution, we can effectively control the amount of overfitting occurring. And the number of seeds necessary is quite small, though this is likely due to the fact that these simulated domains have relatively little noise.

Continuous Action Space. Next we consider overfitting in continuous action spaces using PPO [Schulman et al., 2017] to train the RL on domains from the MuJoCo suite [Todorov et al., 2012] as implemented in the Gym simulator [Brockman et al., 2016]. We consider the 11-dim state space for Reacher and 23-dim state space Thrower. Reacher consists of two links with the task of reaching a goal point, while Thrower consists of an agent attempting to throw a ball into a goal box. In both environments, the goal is initialized randomly for each seed (training and test).

Figure 3 shows that the RL achieves good generalization in the Reacher, but suffers from overfitting in the Thrower with small numbers of training seeds. However at 5 training seeds and more the policy learns to generalize to unseen goal locations (as evaluated over 100 test goals).

²Note that with a single training seed, the initial state drawn is always the same. However, the number of states seen during training is still $|\mathcal{A}|^{|e|}$ where $|e|$ is the length of episode e when using a discrete action space.

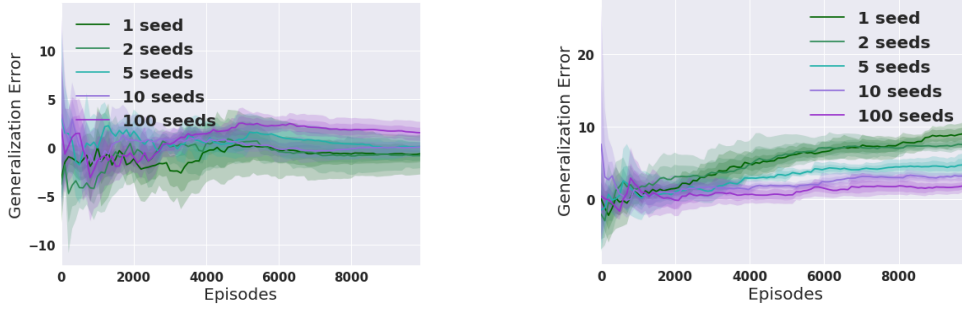


Figure 2: 4-dim Cartpole (left), Pixel Cartpole (right), varying number of train seeds with $\gamma = 0.995$. Averaged over 5 runs. 10K episodes.

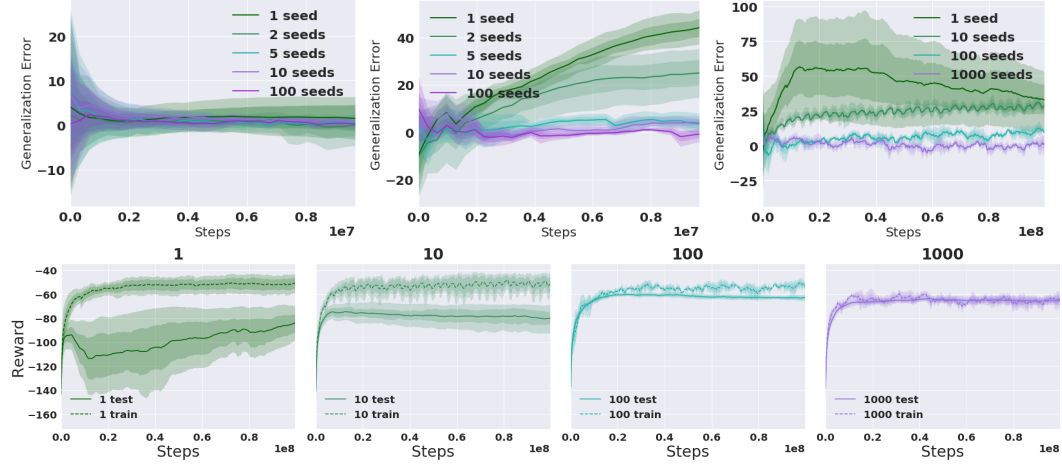


Figure 3: Reacher (top left), Thrower (top center), ThrowerMulti (top right), varying number of train seeds with $\gamma = 0.99$. Averaged over 5 runs. Trained with 10M steps each. Expanded view of reward for ThrowerMulti (bottom).

In addition, we consider a modified Thrower environment (ThrowerMulti): instead of a single goal box, there are now 5 goal boxes placed in random locations. The state now includes a goal id which designates which goal is the correct one – reaching the others provides no reward. The goal of this modification is to check whether the number of seeds necessary grows with the task complexity. Indeed, as shown in Fig. 3, we need a larger number of training seeds to achieve good performance. With the addition of a single free variable, ThrowerMulti now exhibits overfitting even in the 100 seed case. We also clearly see in the 1 seed case that the policy first learns a simple policy that performs slightly better for evaluation, but over time overfits to the train case, causing evaluation performance to drop. The performance on the test seeds for ThrowerMulti is also very high variance compared to that on training seeds and compared to that on the original Thrower domain.

Natural Images. We also evaluate for overfitting in natural images with a pixel-by-pixel reinforcement learning task. We use MNIST LeCun and Cortes [2010] and CIFAR10 Krizhevsky et al., creating an exploration task where an agent is always spawned in the center of a masked image. The state consists of the agent’s position and the 28x28 masked image. At each time step, the agent can move left, right, up, or down, which reveals a square window w of the image. After each time step the agent classifies what the masked image is, and episode ends with reward 1 when it classifies the image successfully. Otherwise it fails after a maximum 100 time steps. We compare against a baseline where it is given the entire image to classify at the end of each episode. MNIST and CIFAR10 results are given in Figure 4.

With natural images, we see even in the 10k training seed case (trained on 10k images), there is a generalization gap. If we compare this with the baseline we see more overfitting effect, since there are now multiple possible partially masked images that correspond to a single image. We see similar effects in CIFAR10 results in Figure 4.

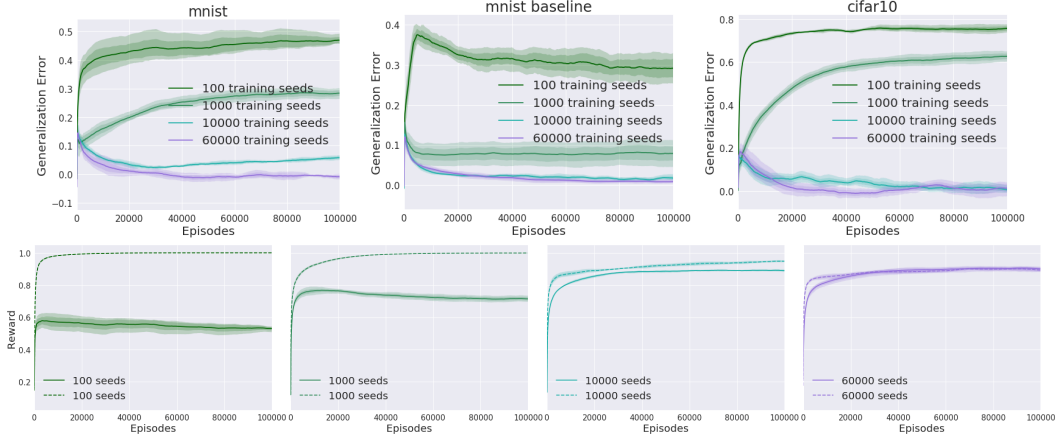


Figure 4: Generalization gap for MNIST (top left) and MNIST baseline (top center) where number of seeds corresponds to number of unique images. Total reward given for MNIST (bottom). Window size $w = 5$. CIFAR10 result (top right) with $w = 10$.

4.2 On memorization in RL: a randomized reward test

The phenomenon of memorization in supervised learning is examined by assigning random labels to training examples [Zhang et al., 2018, Arpit et al., 2017]. This does not extend directly to the RL setting. Instead, we propose to examine memorization by injecting randomness into the reward function. In most continuous domains, the reward varies relatively smoothly over the state space, or at least there are few discontinuities (e.g. when reaching a goal area). By randomizing the reward function, we can examine whether RL models exhibit memorization and learn spurious patterns that will not generalize. When there are few perturbations to the reward, or there are many training seeds, the policy should still be able to learn the given reward signal. However, when the reward function becomes more erratic, it should be more difficult for the policy to train and to generalize well.

To create randomized reward functions, we bin the state space into k equal bins. For each bin, we uniformly at random choose a reward multiplier β between $[-1, 1]$. These multipliers are deterministic – they are consistent for a specific seed, but different across different initial states s_0 . We control the amount of randomness injected into the environment with a parameter p_{rand} , where p_{rand} is the probability of each bin having its reward signal modified by the multiplier.

Discrete Action Space. Figure 5 shows $k = 3$ bins for Cartpole with a single train seed (top) and 100 train seeds (bottom). The model is trained on random reward with train seeds, with $p_{\text{rand}} \in [0.1, 0.2, 0.5, 1]$. In this case we see performance start to drop off as p increases. For low p_{rand} , the model is able to effectively ignore the noise. In the 1 seed case we see the model successfully learn the random reward, especially noticeable in the $p_{\text{rand}} = 0.5$ and $p_{\text{rand}} = 1.0$ columns. However, the model does not have the capacity to memorize all the random rewards even in the 100 seed case, and so it only learns the true reward signal up until performance collapses when $p_{\text{rand}} = 1.0$, where there is no true reward signal left and the random reward is too complex to learn³. Additional results for the Acrobot domain can be found in Appendix B.2.

Continuous Action Space. Figure 6 shows results for Thrower with randomized rewards. Again we see that it is easy to memorize the random reward in the 1 seed case, but much harder in the 100 seed case, and so it instead learns to concentrate on the true reward signal. We observe much larger variance in the single training seed case. Similar results for Reacher can be found in Appendix B.3.

Natural Images. Figure 7 shows results for MNIST with randomized labels. As p increases we see inability to generalize to the test set, but that we can still achieve perfect memorization on the training set. We had to increase the capacity of the model and use a ResNet-18 He et al. [2015] as backbone to achieve perfect memorization on the 10k train set.

³Note that in the Cartpole environment any policy that can find positive reward (even random reward) and optimize for it will also perform well on the original task – the family of policies for the original environment is a superset of policies for any reward function with a positive signal that incentivizes prolonging the episode.

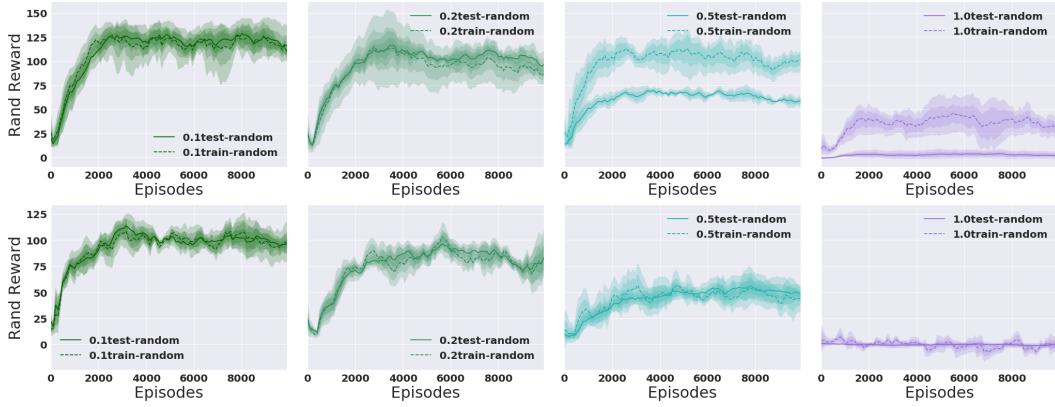


Figure 5: $k = 3$. Full experiments on randomizing reward on 4-dim Cartpole: Varying p_{rand} (cols) with $\gamma = 0.995$ and 1 training seed (top), 100 training seeds (bottom). Averaged over 5 runs. Models are trained on the random reward and evaluated on the original reward.

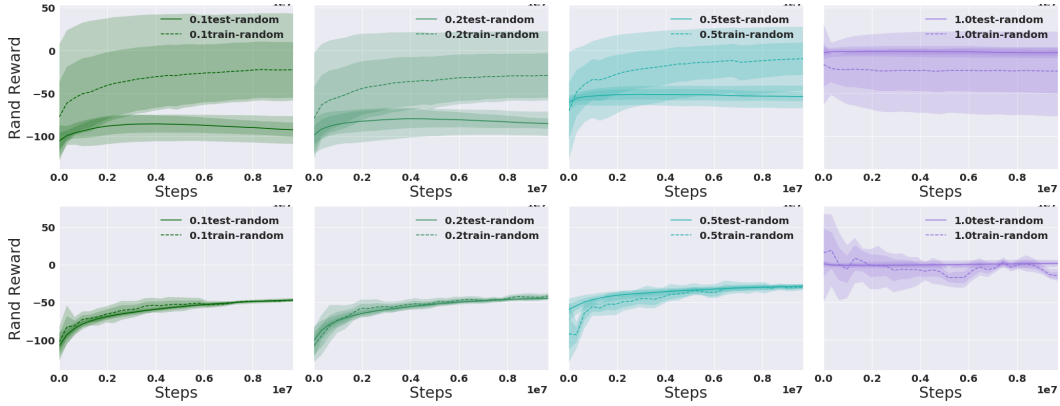


Figure 6: Thrower, varying p_{rand} of each bin randomized with $k = 3$ and $\gamma = 0.99$. Averaged over 5 runs. 1 seed (top), 100 seeds (bottom).*

*Reward values are not directly comparable across columns because the percentage of bins modified by the random multiplier changes the average reward obtained by a random policy.

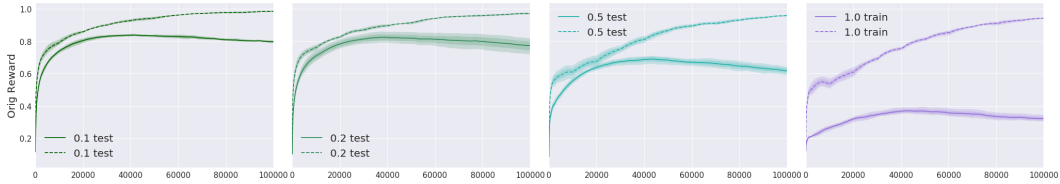


Figure 7: Train and test performance with increasing p from left to right on MNIST 10k. Window size $w = 5$.

5 The out-of-task case for generalization in RL

Moving beyond the case where noise is induced only via the random seed, we now consider cases where it is valuable to generalize over possible distributional shifts between training and evaluation conditions. This is closer to the case considered in previous work on overfitting in RL [Whiteson et al., 2011, Zhang et al., 2018], and in the broadest sense extends to notions of transfer [Taylor and Stone, 2009] and zero/few-shot learning [Oh et al., 2017].

We consider the cases where the state and action sets are the same, but noise may induce changes in transition dynamics, reward function, or initial state distribution. There is evidence (in the discrete state setting) that if the number of tasks you train on is not varied enough, the model tends to memorize the specific environments and learn them explicitly [Zhang et al., 2018]. When trained on enough environments, we expect generalization to allow the RL agent to navigate efficiently on new test environments drawn from the same distribution.

Recall that our goal is not to study transfer broadly, but to examine notions of overfitting and generalization in realistic conditions. Thus we consider two mechanisms for injecting noise into the domain. First we consider an expansion of the initial state distribution, which we implement by applying a multiplier to the initial state chosen. In the MuJoCo domains, the state is initialized uniformly at random from a given range for each dimension. We want to evaluate a specific shift where we train with initial state distribution $\mathcal{S}_{\text{train},0}$ and evaluate with different initial state distribution $\mathcal{S}_{\text{test},0}$. We investigate the setting where $\mathcal{S}_{\text{test},0}$ is a strict superset of $\mathcal{S}_{\text{train},0}$, but this evaluation can also occur in sets with no overlap. In practice, we expand this initial state s_0 with a multiplier m to get new initial state $s'_0 = ms_0$. We vary the magnitude of the multiplier m to see the effect of increasing the noise. The results in Table 1 confirm that the generalization improves significantly with more training seeds, but is made more difficult when there is increased noise in the simulation distribution.

ENVIRONMENT	# OF TRAINING SEEDS	MULTIPLIER				
		$m = 1$	$m = 5$	$m = 10$	$m = 20$	$m = 100$
THROWER	1	-101.09	-95.49	-97.24	-101.13	-110.31
	2	-74.59	-77.86	-78.38	-78.37	-84.84
	5	-52.77	-53.58	-54.67	-53.93	-64.51
	10	-53.67	-53.71	-54.10	-56.69	-70.66
	100	-49.68	-49.24	-51.41	-50.32	-58.85

Table 1: Out-of-task generalization on Thrower, reporting the estimated value averaged over 100 test seeds. Columns indicate the multiplier on the initial state.

Second, we evaluate policy robustness by adding Gaussian noise $n \sim \mathcal{N}(0, \sigma^2)$ directly to the observation space. We add zero-mean Gaussian noise with variance σ^2 to each observed state at evaluation, and measure robustness of the policy as we increase σ^2 . The results in Table 2 follow a similar trend as those in Table 1.

ENVIRONMENT	# OF TRAINING SEEDS	VARIANCE OF NOISE		
		$\sigma^2 = 0.$	$\sigma^2 = 0.1$	$\sigma^2 = 0.2$
THROWER	1	-99.1	-106.0	-114.8
	2	-74.4	-84.8	-100.0
	5	-52.3	-69.0	-106.3
	10	-52.7	-72.6	-103.0
	100	-49.8	-64.2	-93.7

Table 2: Transfer experiments on Thrower. Columns indicate the variance σ^2 of the Gaussian noise added to the observation space.

6 The effect of model-based RL

Several claims have been made about the fact that model-based RL improves robustness of results. We therefore finish our investigation by looking into the generalization abilities of model-based RL methods (Fig. 8). We consider a Double DQN architecture with an additional two heads that output a prediction of next state and reward (in addition to Q-value). We consider the same modification to the critic to transfer PPO into a model-based approach.

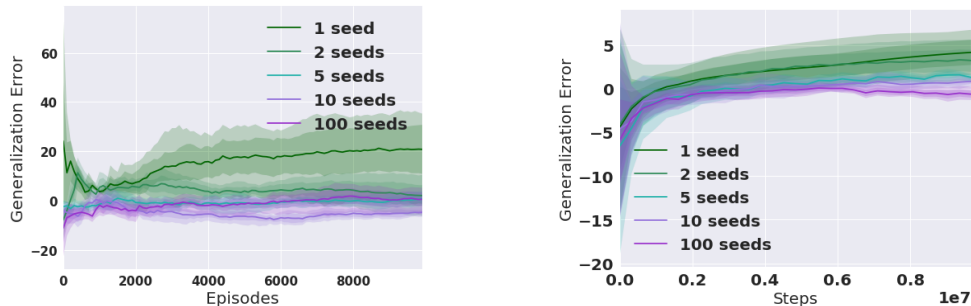


Figure 8: Model-based Reacher (left), and Thrower (right). Varying number of train seeds from 1 to 100 with $\gamma = 0.99$. Averaged over 5 runs.

Results suggest that explicitly learning the dynamics model compounds existing bias in the data in the limited training seed regime. We invite the reader to examine Figure 8 and compare with the model-free results in Figure 3. We see that Reacher now exhibits generalization error in the model-based case where it did not in the model-free case, and the generalization gap has increased for Thrower.

7 Related Work

While not as prevalent as in the SL case, there has been some work exploring evaluation of generalization and overfitting in RL. Rajeswaran et al. [2017] show with linear and RBF parameterizations that they can achieve surprisingly good generalization compared to more elaborate parameterizations, and thus call for simpler linear models for better generalization. However, this is unrealistic for tasks with highly complex dynamics or nonlinear mapping between the state and value space. Francois-Lavet et al. [2017] also looks at overfitting in the batch reinforcement learning case in POMDPs (Partially Observable Markov Decision Processes), specifically exploring the bias-variance tradeoff in the limited data scenario. They are limited to the batch setting in order to control the number of samples, but we look at the limited data setting by controlling the number of seeds, and therefore can still analyze online approaches.

Murphy [2005] analyzes generalization error for Q-learning with function approximation in the batch case. They define generalization error as the average difference in value when using the optimal policy as compared to using the greedy policy based on the learned value function. This requires knowing the optimal policy, which is infeasible in many environments. Ponsen et al. [2010] is a survey of abstraction and generalization in RL and also touches upon the notion of transfer as generalization.

Concurrent work [Zhang et al., 2018] shows memorization in reinforcement learning in the discrete domain with gridworld experiments. Our analysis focuses on continuous domains with effectively infinite number of states, which can be more complex and closer to many real world settings.

8 Conclusion

Currently, much RL work is still being done in simulation, with the goal of eventually transferring methods and policies to the real world. Of course we know that simulated environments lack the diversity – complex signal, natural noise, nonstationary stochasticity – of real world environments. Our natural image experiments show the discrepancy in number of seeds required for true generalization compared to the simulation environments. But until we drastically improve the sample complexity of RL methods, developing and testing in simulation will remain common. Simulated environments also continue to be a necessary tool as a controllable benchmark to compare methods, since it is not possible to “share the real world.”

Given this state of affairs, we have conducted a thorough investigation into the pitfalls of overfitting in continuous RL domains. We present a methodology for detecting overfitting, as well as evaluation metrics for within-task and out-of-task generalization. Especially in robotics tasks where it is infeasible to train on the same distribution as evaluation, our work shows the discrepancy in performance that we can expect to see in transfer scenarios. This methodology also decouples

evaluation of generalization from sample complexity for online methods. As deep reinforcement learning gains more traction and popularity, and as we increase the capacity of our models, we need rigorous methodologies and agreed upon protocols to define, detect, and combat overfitting. Our work contains several simple useful lessons that RL researchers and practitioners can incorporate to improve the quality and robustness of their models and methods.

References

- D. Arpit, S. Jastrzebski, N. Ballas, D. Krueger, E. Bengio, Kanwal M.S., T. Maharaj, A. Fischer, A. Courville, Y. Bengio, and S. Lacoste-Julien. A closer look at memorization in deep networks. In *ICML*, 2017.
- Charles Beattie, Joel Z. Leibo, Denis Teplyashin, Tom Ward, Marcus Wainwright, Heinrich Küttler, Andrew Lefrancq, Simon Green, Víctor Valdés, Amir Sadik, Julian Schrittwieser, Keith Anderson, Sarah York, Max Cant, Adam Cain, Adrian Bolton, Stephen Gaffney, Helen King, Demis Hassabis, Shane Legg, and Stig Petersen. Deepmind lab. *CoRR*, abs/1612.03801, 2016.
- R. Bellman. A Markovian Decision Process. *Journal of Mathematics and Mechanics*, 1957.
- Greg Brockman, Vicki Cheung, Ludwig Pettersson, Jonas Schneider, John Schulman, Jie Tang, and Wojciech Zaremba. Openai gym, 2016.
- V. Francois-Lavet, D. Ernst, and R. Fonteneau. On overfitting and asymptotic bias in batch reinforcement learning with partial observability. *ArXiv e-prints*, September 2017.
- Kaiming He, Xiangyu Zhang, Shaoqing Ren, and Jian Sun. Deep residual learning for image recognition. *CoRR*, abs/1512.03385, 2015.
- P. Henderson, R. Islam, and Pineau J. Precup D. Meger D. Bachman, P. Deep reinforcement learning that matters. In *AAAI*, 2018.
- Diederik P. Kingma and Jimmy Ba. Adam: A method for stochastic optimization. *CoRR*, abs/1412.6980, 2014.
- Alex Krizhevsky, Vinod Nair, and Geoffrey Hinton. Cifar-10 (canadian institute for advanced research). URL <http://www.cs.toronto.edu/~kriz/cifar.html>.
- Yann LeCun and Corinna Cortes. MNIST handwritten digit database. 2010. URL <http://yann.lecun.com/exdb/mnist/>.
- Marlos C. Machado, Marc G. Bellemare, Erik Talvitie, Joel Veness, Matthew J. Hausknecht, and Michael Bowling. Revisiting the arcade learning environment: Evaluation protocols and open problems for general agents. *CoRR*, abs/1709.06009, 2017.
- Volodymyr Mnih, Koray Kavukcuoglu, David Silver, Andrei A. Rusu, Joel Veness, Marc G. Bellemare, Alex Graves, Martin Riedmiller, Andreas K. Fidjeland, Georg Ostrovski, Stig Petersen, Charles Beattie, Amir Sadik, Ioannis Antonoglou, Helen King, Dharshan Kumaran, Daan Wierstra, Shane Legg, and Demis Hassabis. Human-level control through deep reinforcement learning. *Nature*, 518(7540):529–533, 02 2015. URL <http://dx.doi.org/10.1038/nature14236>.
- Susan A. Murphy. A generalization error for q-learning. *J. Mach. Learn. Res.*, 6:1073–1097, December 2005. ISSN 1532-4435. URL <http://dl.acm.org/citation.cfm?id=1046920.1088709>.
- J. Oh, S. Singh, H. Lee, and P. Kohli. Zero-shot task generalization with multi-task deep reinforcement learning. In *ICML*, 2017.
- Marc Ponsen, Matthew E. Taylor, and Karl Tuyls. Abstraction and generalization in reinforcement learning: A summary and framework. In Matthew E. Taylor and Karl Tuyls, editors, *Adaptive and Learning Agents*, pages 1–32, Berlin, Heidelberg, 2010. Springer Berlin Heidelberg. ISBN 978-3-642-11814-2.
- A. Rajeswaran, K. Lowrey, E. Todorov, and S. Kakade. Towards Generalization and Simplicity in Continuous Control. *ArXiv e-prints*, March 2017.

- John Schulman, Filip Wolski, Prafulla Dhariwal, Alec Radford, and Oleg Klimov. Proximal policy optimization algorithms. *CoRR*, abs/1707.06347, 2017.
- Richard S. Sutton. Generalization in reinforcement learning: Successful examples using sparse coarse coding. In *Advances in Neural Information Processing Systems* 8, pages 1038–1044. MIT Press, 1996.
- M. Taylor and P. Stone. Transfer learning for reinforcement learning domains: A survey. *JMLR*, 2009.
- Emanuel Todorov, Tom Erez, and Yuval Tassa. Mujoco: A physics engine for model-based control. In *IROS*, pages 5026–5033. IEEE, 2012. ISBN 978-1-4673-1737-5. URL <http://dblp.uni-trier.de/db/conf/iros/iros2012.html#TodorovET12>.
- Hado van Hasselt, Arthur Guez, and David Silver. Deep reinforcement learning with double q-learning. *CoRR*, abs/1509.06461, 2015.
- S. Whiteson, B. Tanner, M. E. Taylor, and P. Stone. Protecting against evaluation overfitting in empirical reinforcement learning. In *2011 IEEE Symposium on Adaptive Dynamic Programming and Reinforcement Learning (ADPRL)*, pages 120–127, April 2011. doi: 10.1109/ADPRL.2011.5967363.
- C. Zhang, S. Bengio, M. Hardt, B. Recht, and O. Vinyals. Understanding deep learning requires rethinking generalization. *ArXiv e-prints*, November 2016.
- C. Zhang, O. Vinyals, R. Munos, and S. Bengio. A Study on Overfitting in Deep Reinforcement Learning. *ArXiv e-prints*, April 2018.

A Model Specifications and Hyperparameters

Convolutional head for pixel space consists of 3 convolutional layers with middle dim 512 and ReLU nonlinearities.

A.1 Double DQN

- lr: 3e-3 for low-dim, 3e-4 for pixel
- target update interval: 1000
- replay memory: 1M for low-dim, 100K for pixel
- Architecture: 3-layer MLP with middle dim 512
- γ : 0.995 for Cartpole, 0.99 for Acrobot

A.2 PPO

- lr: 3e-4
- PPO epochs: 10
- Number of steps between updates: 2048
- γ : 0.99
- Batch size: 32
- Architecture: 3-layer MLP with middle dim 512

Used Adam Kingma and Ba [2014] as optimizer.

B Environments

B.1 Cartpole

B.1.1 Random Reward

The random reward is binning the angle θ of the pole. Each bin has a probability p of having a randomized reward with its own random multiplier between -1 and 1.

4-Dim Cartpole Full randomized reward experiments varying the number of training seeds, number of bins b , and randomization probability p .

Figure 9 shows random rewards on Cartpole with $k = 3$ bins and varying the probability $p \in [0.1, 0.2, 0.5, 1]$, with evaluation done with the original reward. This experiment is done on the original 4-dimensional state space for Cartpole. The original reward function of Cartpole returns a reward of 1 at every step, so we see that we still get enough positive reward signal for the original Cartpole to perform quite well even when all k bins are assigned a random multiplier.

Number of episodes: 10K

Pixel Cartpole Full randomized reward experiments varying the number of training seeds, number of bins b , and randomization probability p .

Number of episodes: 10K Replay memory: 100K (s, a, r, s') tuples Learning rate: 3e-4

B.2 Acrobot

Acrobot is a 2-link pendulum with only the second joint actuated. It is instantiated with both links pointing downwards. The goal is to swing the end-effector at a height at least the length of one link above the base.

The state consists of the $\sin()$ and $\cos()$ of the two rotational joint angles θ_1, θ_2 and the joint angular velocities.

$$[\cos(\theta_1) \sin(\theta_1) \cos(\theta_2) \sin(\theta_2) \dot{\theta}_1 \dot{\theta}_2] \quad (4)$$

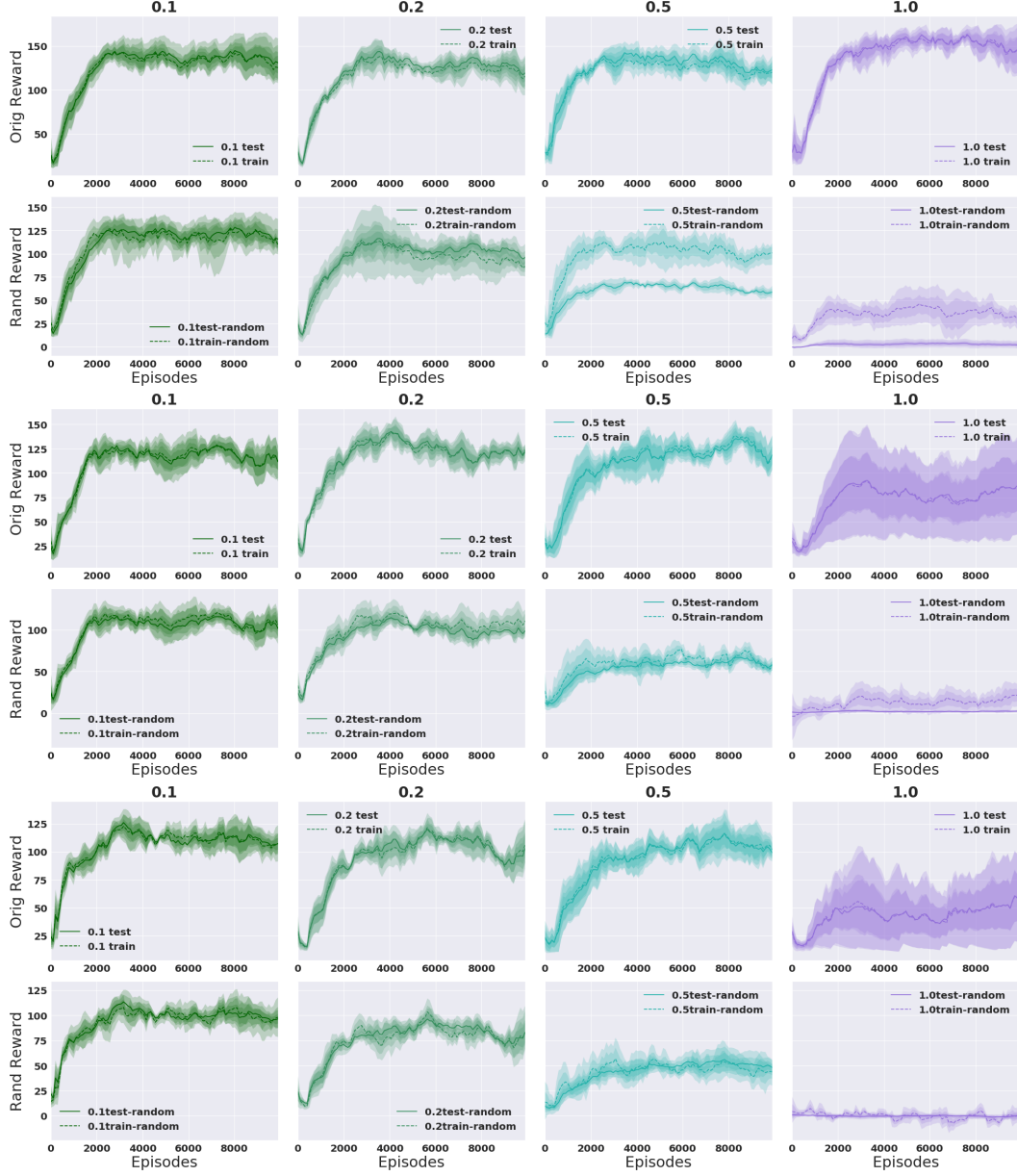


Figure 9: $b = 3$. Full experiments on randomizing reward on 4-dim Cartpole: Varying p (cols) with $\gamma = 0.995$ and varying 1, 10, 100 training seeds (rows). Averaged over 5 runs.

For the first link, an angle of 0 corresponds to the link pointing downwards. The angle of the second link is relative to the angle of the first link. An angle of 0 corresponds to having the same angle between the two links. The action is either applying +1, 0 or -1 torque on the joint between the two pendulum links.

Number of episodes: 10K

B.2.1 Random Reward

We bin θ_0 , the angle of the first link of the pendulum.

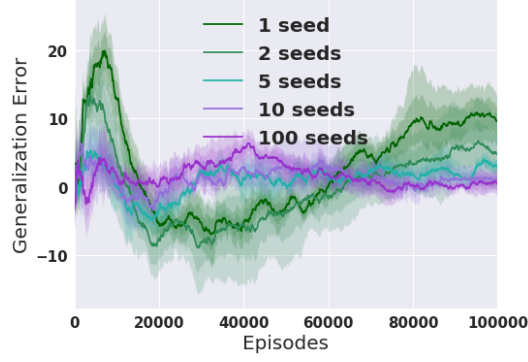


Figure 10: Model-based. Pixel Cartpole. Two states, varying number of train seeds with $\gamma = 0.99$. Averaged over 5 runs.

B.3 Reacher

Reward on a log scale. (negated, log, then negated again)
Number of frames: 10M

B.3.1 Random Reward

For Reacher, we randomize reward by binning θ , the angle of the first link.

B.4 Thrower

Number of frames: 100M

B.4.1 Random Reward

We bin the first dimension of the observation space.

C Transfer

ENVIRONMENT	SEED	$\sigma^2 = 0.$	$\sigma^2 = 0.0001$	$\sigma^2 = 0.0005$	$\sigma^2 = 0.001$	$\sigma^2 = 0.002$
CARTPOLE	1	89.7	90.3	75.5	47.4	26.7
	2	131.3	131.3	112.9	69.5	35.4
	5	105.7	102.7	66.6	39.1	19.2
	10	145.5	144.1	122.8	101.5	78.8
	100	122.4	119.9	99.7	66.8	35.8
		$\sigma^2 = 0.$	$\sigma^2 = 0.1$	$\sigma^2 = 0.2$	$\sigma^2 = 0.3$	$\sigma^2 = 0.4$
PIXEL CARTPOLE	1	19.4	19.2	18.8	18.9	19.6
	2	20.3	18.2	17.9	18.3	19.1
	5	22.5	20.0	20.2	20.3	20.4
	10	16.4	19.8	20.6	20.6	20.2
	100	21.7	17.4	17.3	17.4	18.0
		$\sigma^2 = 0.$	$\sigma^2 = 0.001$	$\sigma^2 = 0.002$	$\sigma^2 = 0.003$	$\sigma^2 = 0.004$
PIXEL CARTPOLE (MODEL BASED)	1	31.4	34.2	17.9	16.3	15.2
	2	29.5	31.5	17.2	17.2	16.5
	5	35.2	38.2	20.0	21.7	21.3
	10	31.1	35.7	19.7	18.6	18.4
	100	25.2	30.5	18.9	18.5	19.0

Table 3: Transfer experiments on Cartpole and Pixel Cartpole for model-free and model-based. Columns indicate the variance σ^2 of the Gaussian noise added to the observation space. Note the difference in σ^2 of noise for all three settings.

ENVIRONMENT	SEED	$\sigma^2 = 0.$	$\sigma^2 = 0.01$	$\sigma^2 = 0.05$	$\sigma^2 = 0.1$	$\sigma^2 = 0.2$
ACROBOT	1	-130.4	-132.1	-156.8	-185.7	-198.6
	2	-118.7	-120.0	-170.8	-193.1	-199.0
	5	-95.0	-98.8	-137.2	-174.5	-193.1
	10	-100.6	-100.4	-134.9	-172.6	-196.2
	100	-107.5	-111.9	-155.1	-182.8	-196.8
		$\sigma^2 = 0.$	$\sigma^2 = 0.001$	$\sigma^2 = 0.002$	$\sigma^2 = 0.003$	$\sigma^2 = 0.004$
PIXEL ACROBOT	1	-128.1	-129.6	-198.9	-199.9	-200.0
	2	-109.8	-109.2	-199.9	-200.7	-200.7
	5	-87.2	-89.0	-200.2	-199.8	-200.2
	10	-96.8	-97.6	-199.9	-199.6	-200.2
	100	-83.6	-84.7	-200.3	-199.9	-200.7

Table 4: Transfer experiments on Acrobot. Columns indicate the variance σ^2 of the Gaussian noise added to the observation space.

ENVIRONMENT	SEED	$\sigma^2 = 0.$	$\sigma^2 = 0.1$	$\sigma^2 = 0.2$	$\sigma^2 = 0.5$	$\sigma^2 = 1.$
REACHER	1	-11.3	-11.8	-12.1	-13.5	-15.2
	2	-27.2	-27.1	-26.1	-24.	-24.6
	5	-13.8	-14.9	-15.5	-16.7	-18.8
	10	-11.8	-11.7	-12.1	-13.8	-13.7
	100	-11.4	-11.4	-11.7	-12.7	-14.3

Table 5: Transfer experiments on Reacher. Columns indicate the variance σ^2 of the Gaussian noise added to the observation space.

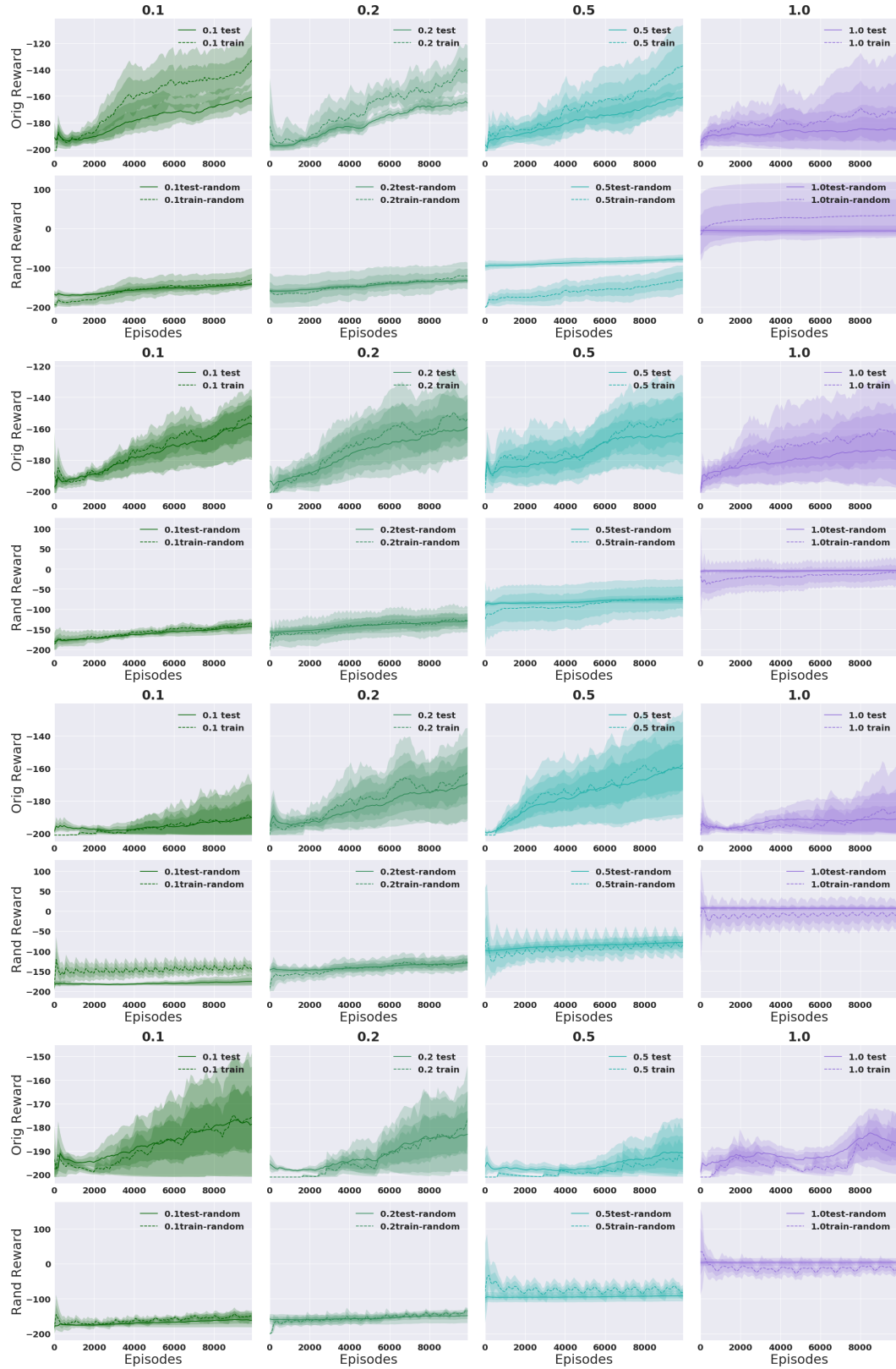


Figure 11: $b = 3$. Full experiments on randomizing reward on Acrobot: Varying p (cols) with $\gamma = 0.99$ and varying 1, 2, 5 and 10 training seeds (rows). Averaged over 5 runs. 100K episodes.

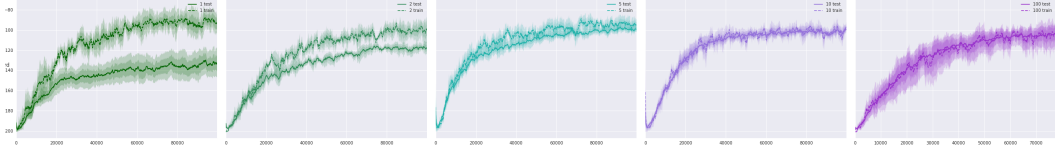


Figure 12: Reward for Acrobot varying number of training seeds. Averaged over 5 runs.

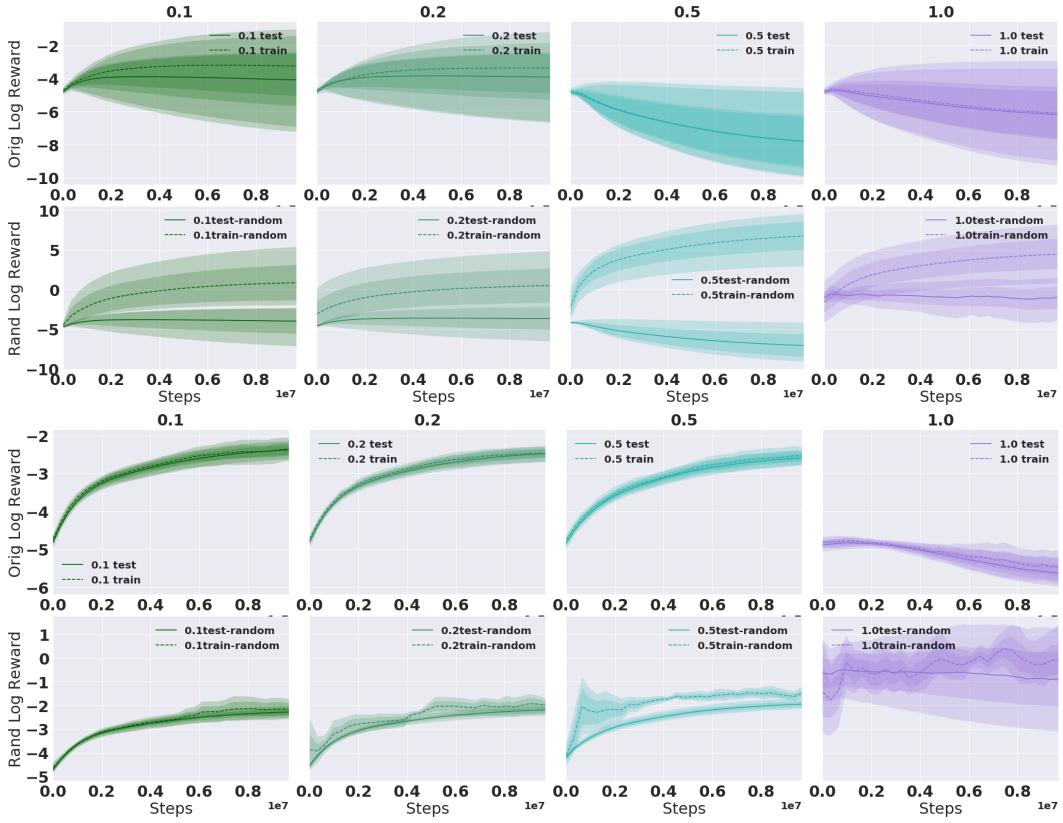


Figure 13: $b = 3$. Full experiments on randomizing reward on Reacher: Varying p (cols) with $\gamma = 0.99$ and 1 and 100 training seed (rows). Averaged over 5 runs.

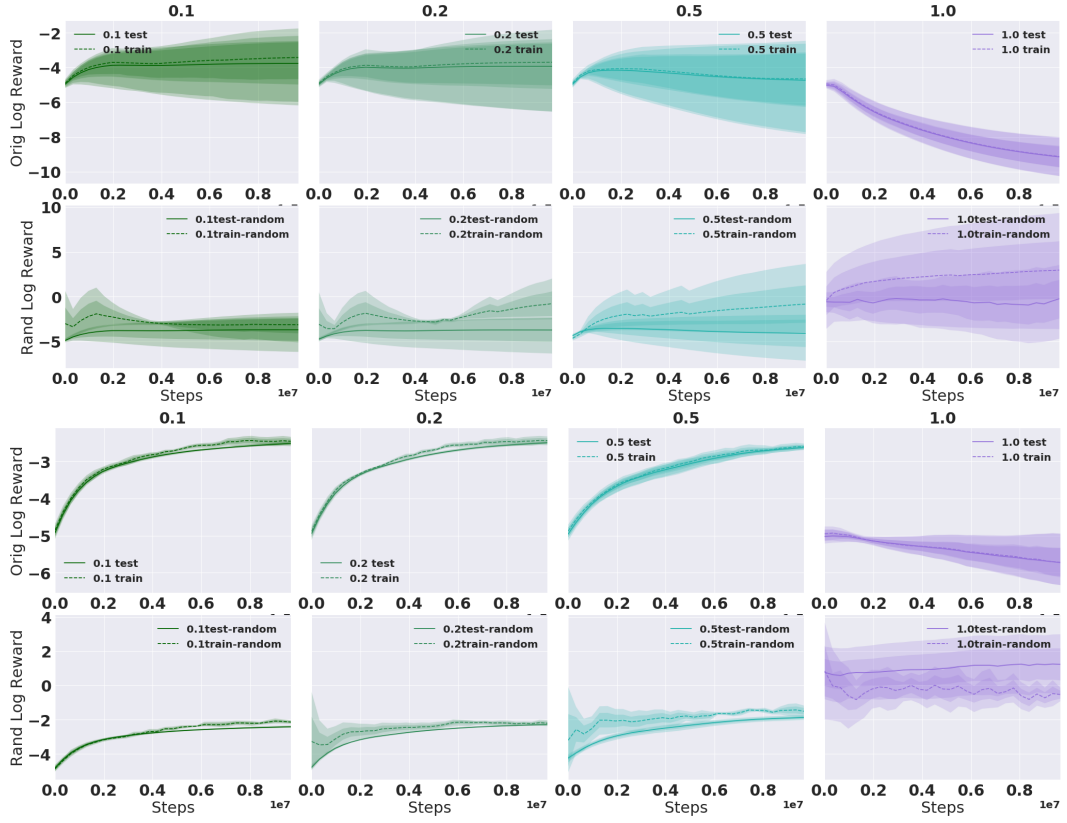


Figure 14: $b = 3$. Full experiments on randomizing reward on model-based Reacher: Varying p (cols) with $\gamma = 0.99$ and 1 and 100 training seeds (rows). Averaged over 5 runs.

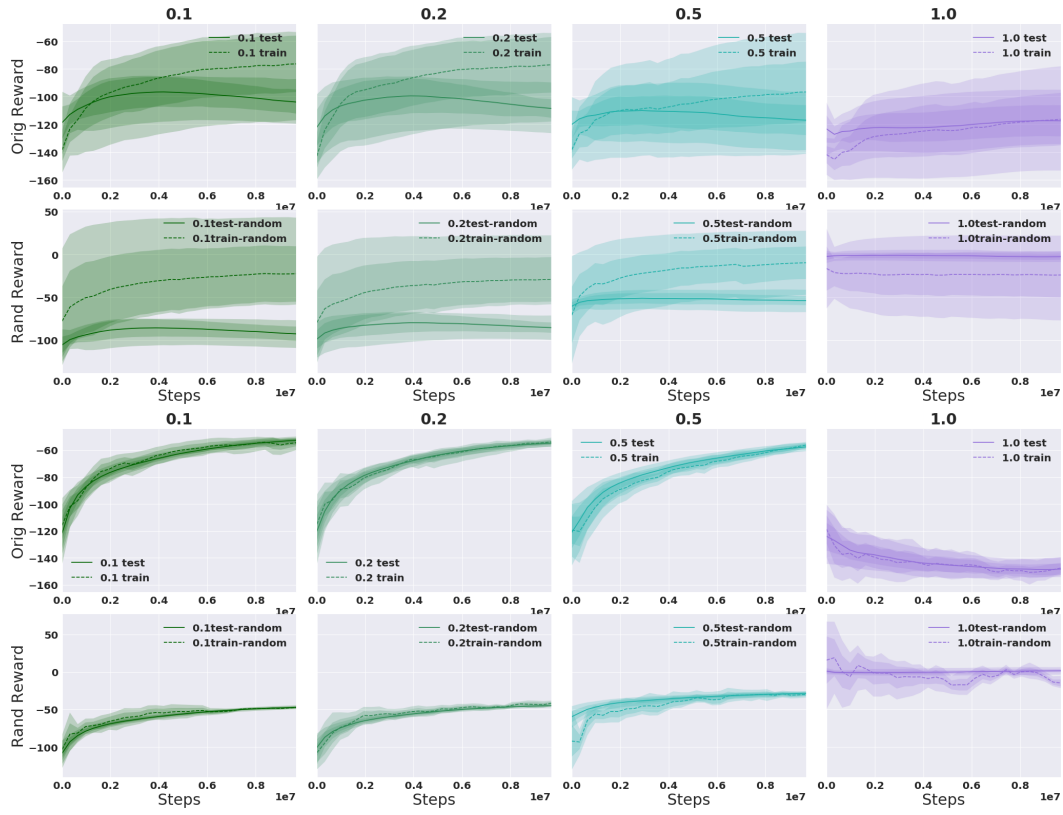


Figure 15: $k = 3$. Full experiments on randomizing reward on Throwing: Varying p (cols) with $\gamma = 0.99$ and 1 and 100 training seeds. Averaged over 5 runs.

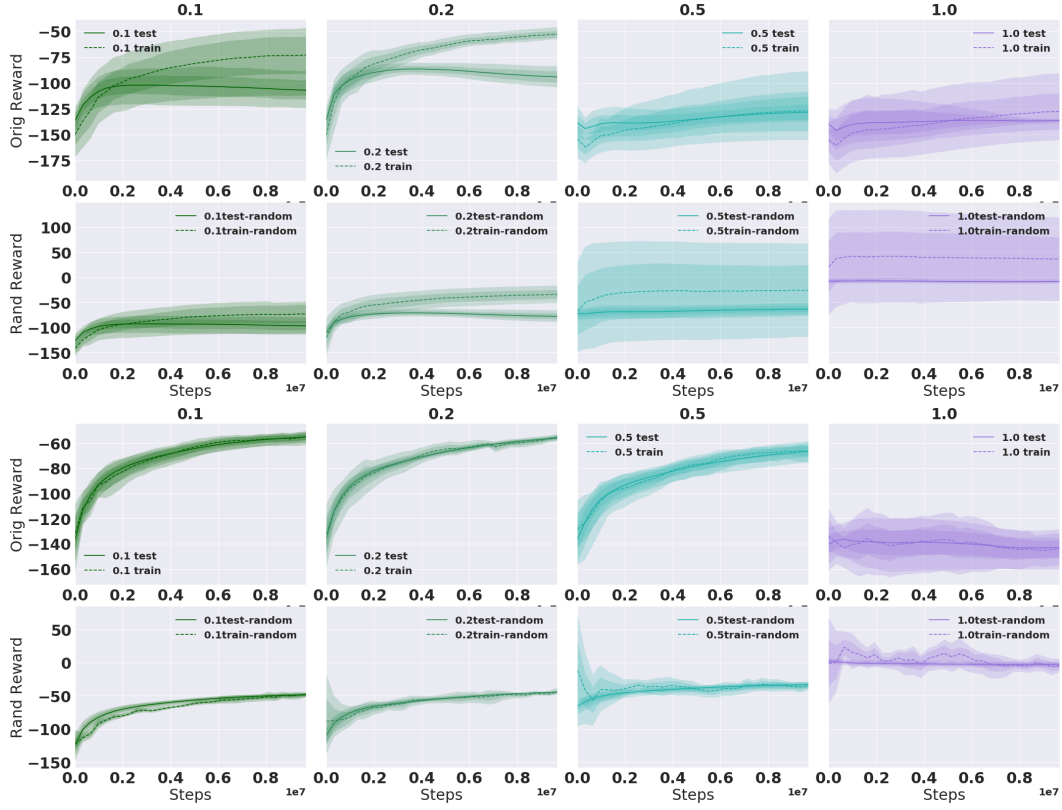


Figure 16: $b = 3$. Full experiments on randomizing reward on model-based Throwing: Varying p (cols) with $\gamma = 0.99$ and 1 and 100 training seeds (rows). Averaged over 5 runs.